J. Cell. Mol. Med. Vol 14, No 1-2, 2010 pp. 290-302

Genetic transfer of fusion proteins effectively inhibits VCAM-1-mediated cell adhesion and transmigration *via* inhibition of cytoskeletal anchorage

Christoph E. Hagemeyer [a,*,#], Ingo Ahrens [a,b,#], Nicole Bassler [a], Natia Dschachutaschwili [a,b], Yung C. Chen [a], Steffen U. Eisenhardt [a,c], Christoph Bode [b], Karlheinz Peter [a]

[a] *Centre for Thrombosis and Myocardial Infarction, Baker Heart Research Institute, Melbourne, Australia*
[b] *Department of Cardiology and Angiology, University of Freiburg, Germany*
[c] *Department of Plastic and Handsurgery, University of Freiburg Medical Centre, Freiburg, Germany*

Received: September 16, 2008; Accepted: May 26, 2008

Abstract

The adhesion of leukocytes to endothelium plays a central role in the development of atherosclerosis and thus represents an attractive therapeutic target for anti-atherosclerotic therapies. Vascular cell adhesion molecule-1 (VCAM-1) mediates both the initial tethering and the firm adhesion of leukocytes to endothelial cells. Our work evaluates the feasibility of using the cytoskeletal anchorage of VCAM-1 as a target for gene therapy. As a proof of concept, integrin $\alpha_{IIb}\beta_3$-mediated cell adhesion with clearly defined cytoskeletal anchorage was tested. We constructed fusion proteins containing the intracellular domain of β_3 placed at various distances to the cell membrane. Using cell adhesion assays and immunofluorescence, we established fusion constructs with competitive and dominant negative inhibition of cell adhesion. With the goal being the transfer of the dominant negative mechanism towards VCAM-1 inhibition, we constructed a fusion molecule containing the cytoplasmic domain of VCAM-1. Indeed, VCAM-1 mediated leukocyte adhesion can be inhibited *via* transfection of DNA encoding the designed VCAM-1 fusion protein. This is demonstrated in adhesion assays under static and flow conditions using CHO cells expressing recombinant VCAM-1 as well as activated endothelial cells. Thus, we are able to describe a novel approach for dominant negative inhibition of leukocyte adhesion to endothelial cells. This approach warrants further development as a novel gene therapeutic strategy that aims for a locally restricted effect at atherosclerotic areas of the vasculature.

Keywords: VCAM-1 • adhesion molecules • cytoskeletal anchorage • monocyte • endothelium • transmigration

Introduction

Adhesion of mononuclear cells at the site of endothelial inflammation is one of the first steps in the development of atherosclerotic plaques. This adhesion occurs *via* the specific interaction of a number of receptors and ligands [1–3]. The integrin $\alpha_4\beta_1$ (VLA-4) on monocytes is the major ligand for the vascular cell adhesion molecule-1 (VCAM-1, CD106) [4], an immunoglobulin-like endothelial adhesion molecule highly expressed in human atherosclerotic plaques [5] and linked to atherosclerosis susceptibility in mouse models [6]. Although VCAM-1 is structurally similar to ICAM-1, its pattern of regulation is unique [7]. VCAM-1 is not expressed under baseline conditions but is rapidly induced upon endothelial activation [8]. The up-regulation of VCAM-1 under inflammatory conditions (as observed in atherosclerosis) and on atherosclerotic plaques defines VCAM-1 as a highly attractive target for the treatment of atherosclerosis. Indeed, highly specific *in vivo* visualization of atherosclerotic plaques by molecular imaging of VCAM-1 expression has recently been demonstrated in mice [9] and rabbits [10], demonstrating the specificity of VCAM-1 as an atherosclerosis-specific target.

VCAM-1 is not only an important adhesion receptor, but also acts as a signal transducer upon leukocyte binding. VCAM-1 clustering leads to the activation of Rac1, production of reactive oxygen species (ROS), activation of p38 MAPK and to changes in the

[#] These authors contributed equally.
*Correspondence to: Christoph E. HAGEMEYER,
Centre for Thrombosis & Myocardial Infarction, Baker Heart Research Institute, PO Box 6492 St Kilda Road Central, Melbourne, Victoria 8008, Australia.
Tel.: +61 38 532 1494
Fax: +61 38 532 1100
E-mail: hagemeyer@hotmail.com

doi:10.1111/j.1582-4934.2008.00409.x

actin cytoskeleton (*i.e.* stress fibre formation). All of these events have been associated with the increased endothelial permeability induced by VCAM-1 cross-linking [11].

We hypothesized that inactivation of VCAM-1 *via* transfection of genes encoding for fusion proteins that compete with VCAM-1's cytoskeletal anchorage reduces monocyte adhesion to endothelial cells. However, the interaction of VCAM-1 with the cytoskeleton has not been studied very well and tools to study these interactions are not readily available. In contrast to this, in another family of adhesion molecules, the integrins, the interaction with the cytoskeleton has been well described and proven tools to study this interaction are available [12]. Particularly for the platelet integrin $\alpha_{IIb}\beta_3$ (CD41/CD61) the interaction with the cytoskeleton has been well characterized and we have previously visualized this interaction with immunofluorescence microscopy in the form of adhesion plaque and actin stress fibre formation [13–16]. Since VCAM-1 does not localize to adhesion plaques and does not mediate typical stress fibre formation, the visualization of its cytoskeletal interaction is not possible by immunofluorescence micropscopy. Therefore, we used the interaction of the integrin $\alpha_{IIb}\beta_3$ with the cytoskeleton as a pilot experimental setup and in a second step we then transferred the outcome of this pilot study to an approach aiming at the targeted interruption of VCAM-1's cytoskeletal anchorage.

In order to interfere with $\alpha_{IIb}\beta_3$ cytoskeletal anchorage, we developed different fusion molecules composed of the intracellular part of β_3 and the extracellular and transmembrane part of CD7 as an inert marker. As a proof of concept, we transfected the developed fusion proteins under the control of a tetracycline-regulated expression system into wild-type and $\alpha_{IIb}\beta_3$-expressing CHO cells and investigated their adhesive properties. Based on the results with the various CD7/β_3 fusion molecules, a CD7/VCAM-1 fusion molecule was designed containing the intracellular part of VCAM-1 and the extracellular and transmembrane part of CD7 in order to interfere with the cytoskeletal anchorage of VCAM-1 in a dominant negative manner. The functional consequences of transfection with the generated fusion protein were investigated in a CHO cell model, as well as in primary and immortalized endothelial cells (HUVEC and HMEC).

The aim of our study was to investigate the feasibility of a gene therapy approach, specifically targeting the cytoskeletal anchorage of VCAM-1. Since monocyte recruitment into atherosclerotic plaques causes disease progression, blocking of monocyte adhesion to the vessel wall by local transfection of endothelial cells with a gene expressing a functional blocker of VCAM-1 may offer a novel therapeutic approach for the local treatment of atherosclerosis in coronary and carotid arteries. With the aim to prevent further progression of coronary atherosclerosis, local injection of an adenovirus containing a VCAM-1 inactivating gene into the coronary arteries could be performed in the cardiac catheter laboratory and may be feasible for human application. Local gene delivery by adenovirus vector systems has already been successfully employed in animal models [17, 18]. Very recently, the adenoviral delivery of gene vectors was combined with the local delivery *via* a biodegradable coating of stents [19]. This approach was used to prevent restenosis after stenting of atherosclerotic plaques [19]. Overall, besides the local injection into the coronary arteries, stent-associated delivery may also be useful in general to deliver therapeutic genes with anti-atherosclerotic effects in interventional cardiology.

Materials and methods

Reagents and antibodies

Anti-CD106, anti-CD106-PE (Clone 51-10C9) and CD45-FITC (Clone HI30) were from Becton Dickinson (BD, Franklin Lakes, NJ, USA); anti-CD49d (Clone HP2/1), anti-CD54 (Clone 84H10), anti-CD7 (Clone 8H8) and anti-CD14-PE (Clone RMO52) were from Beckman Coulter (Fullerton, CA, USA); anti-CD62E and anti-CD62E-FITC (Clone BBIG-E4/5) were from R&D Systems (Minneapolis, MN, USA); anti-CD7-FITC (Clone WM31) was from Millipore (Billerica, MA, USA); anti-CD54-FITC (Clon15.2) was from Chemicon (Billerica, MA, USA). Fibrinogen, cytochalasin D and phalloidin-TRITC were from Sigma-Aldrich (St. Louis, MO, USA); MCP-1 was from R&D Systems (Minneapolis, MN, USA), and Calcein AM from Invitrogen (Carlsbad, CA, USA). FITC-labeled goat anti-mouse IgG antibody was from Jackson Immunoresearch (West Grove, PA, USA). ReoPro (abciximab) was from Eli Lilly (Indianapolis, IN, USA).

Cells and cell culture

CHO-K1 cells were purchased from DSMZ (Braunschweig, Germany) and grown in DMEM with 100 U/ml penicillin, 100 μg/ml streptomycin, 0.3 mg/ml L-glutamine, 10% FCS (all from Serva, Heidelberg, Germany). The CHO cell line expressing $\alpha_{IIb}\beta_3$ was established previously [13]. The CHO-AA8 cell line with integrated regulation plasmid pTet Off™ was used according to the supplier's manual (Clontech, Mountain View, CA, USA). ICAM-1 expressing CHO cells were a gift from A. Duperray, Institute Albert Bonniot, La Tronche Cedex, France. E-selectin expressing CHO cells were available in our lab. VCAM-1, CD7/β_3 and CD7/VCAM-1 expressing CHO cells were established by transfection and limited dilution followed by subcloning and cell sorting. Transfected cells were cultured in the presence of G418-sulphate (100–700 μg/ml), Hygromycin (600 μg/ml) or Zeocin (600 μg/ml) (all from Invitrogen, Carlsbad, CA, USA).

We used primary (human umbilical vein endothelial cells, HUVECs) as well as immortalized (human microvascular endothelial cell line-1, HMEC-1) endothelial cells. HUVECs were obtained from PromoCell (Heidelberg, Germany) and cultured in 0.5% gelatin-coated culture plates filled with ECGM supplemented with basic human recombinant fibroblast growth factor 1.0 ng/ml, endothelial cell growth supplement/heparin 4 μl/ml, FBS 2%, recombinant human epidermal growth factor 0.1 ng/ml, hydrocortisone 1 μg/ml, amphotericin B 50 ng/ml, gentamicin 50 μg/ml; all from PromoCell (Heidelberg, Germany). HMEC-1 cells were a gift from H. Eltzschig (University of Tübingen, Germany) and were cultured in MCDB 131 medium supplemented with 100 U/ml penicillin, 100 μg/ml streptomycin, 0.3 mg/ml L-glutamine, 10% FCS, 2 ng/ml hydrocortisone, 10 ng/ml epidermal growth factor (all from Invitrogen, Carlsbad, CA, USA). All cell culture work was conducted at 37°C with 95% humidity and up to 5% CO_2 using aseptic techniques.

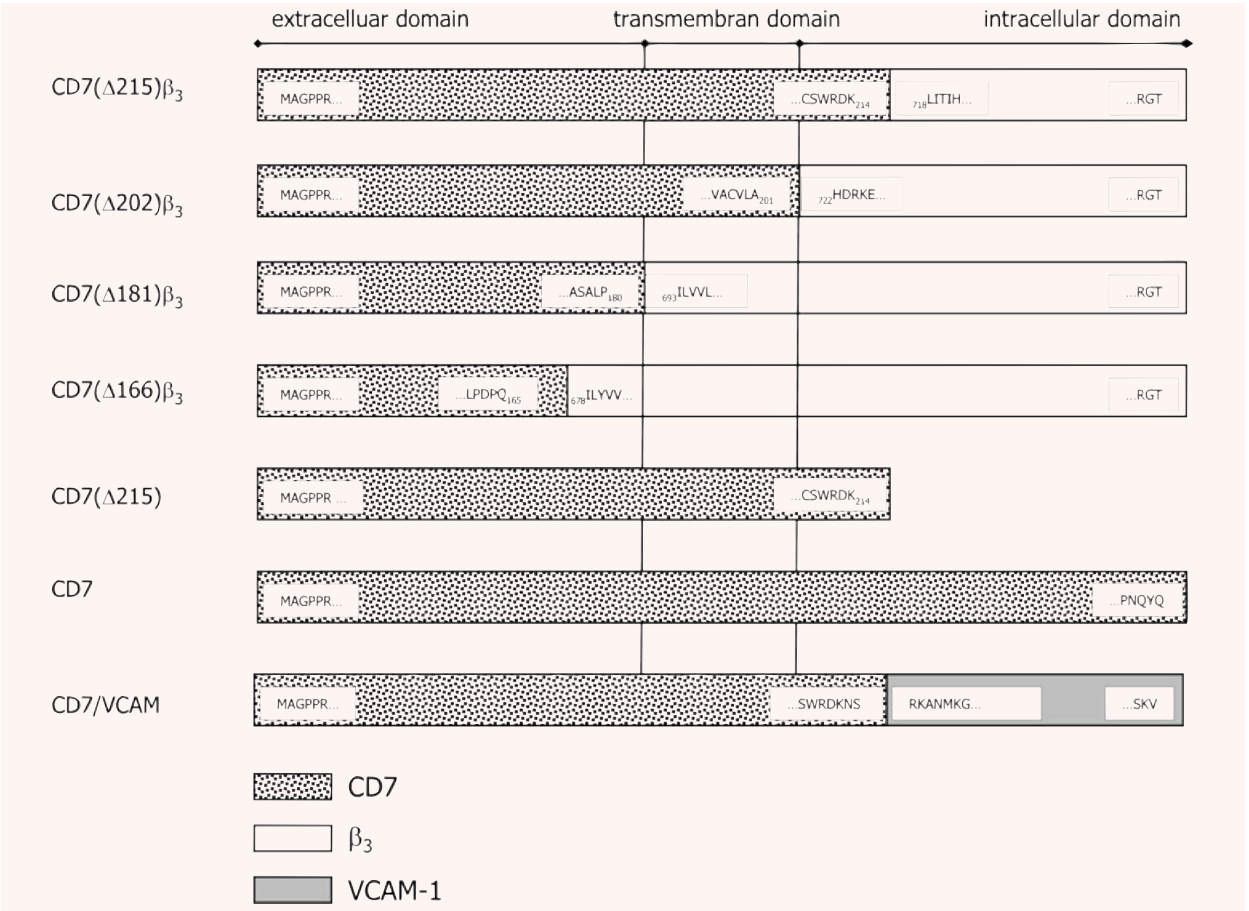

Fig. 1 Overview of generated CD7/β_3 and CD7/VCAM-1 fusion proteins. The sequences of the beginning and the end of the CD7/β_3 and CD7/VCAM-1 protein sequences are depicted. Four different chimeras with different fusion sites between CD7/β_3 and CD7/VCAM-1 and a corresponding control lacking the intracellular part were generated. In addition, native CD7 was used as a control.

Cloning

CD7 (HUGO Gene Nomenclature Committee (HGNC) No 1695) (gift from C. Haller, University of Heidelberg, Germany), VCAM-1 (HGNC:12663) and β_3 (HGNC:6156) (both derived from endothelial cells) cDNA were cloned into pcDNA1 or in pcDM8 plasmid (Invitrogen, Carlsbad, CA, USA). For CD7/β_3 constructs, varying lengths of the cytoplasmatic region of β_3 and the extracellular region of CD7 were generated by fusion-PCR using overlap primers as described earlier [20] and cloned into pUHD10–3 (Manfred Gossen, ZMBH, Heidelberg) (Fig. 1). The cytoplasmic region of VCAM-1 was amplified by PCR with EcoRI and XhoI restriction sites and cut. A part of the intracellular CD7 domain was removed by cutting with EcoRI and XhoI and replaced by the PCR amplified cytoplasmic VCAM part. The fused construct was then subcloned in pZeoSV2(+) (Invitrogen, Carlsbad, CA, USA) and adenovirus vector pTR-UF5 (ProCorde, Munich, Germany) (Fig. 1). Final constructs were confirmed by sequencing. We used the *E. coli* strains SCS 110, XL1-Blue MRF', Epicurian Coli® SURE® (Stratagene, La Jolla, CA, USA), MC 1061/P3, Top10 (Invitrogen, Carlsbad, CA, USA) and Dh5α (BD, Franklin Lakes, NJ, USA). Used primers: Eco-sense-integrin (5′-CCG AAT TCC CTC ATC ACC ATC CAC GAC C-3′); Xba-hind-anti-integrin (5′-CCT CTA GAA GCT TAT CAT TAA GTG CCC CGG TAC-3′); CD7-sense (5′-CCG AAG CTT CTC GAG TCT AGA CCA GAG AGG CTC AGC TGC ACT CGC C-3′); β3-antisense (5′-CCG ACG CGT CTC GAG ACT GCT TAT CAT TAA GTG CC-3′); CD7-β3-overlap (5′-CCT GGG GGT GGC GTG TGT GCT GGT GGC GCA CGA CCG AAA AGA ATT CGC T-3′); CD7-β3-TM-overlap (5′-CCA GCA GCC TCT GCC CTC CCT ATC CTG GTG GTC CTG CTC TCA GTG-3′); CD7-β3-TM-15 overlap (5′-GGC TCC GCC CTC CCT GAC CCG CAG ATC CTG TAT GTG GTA GAA GAG CC-3′).

Peripheral blood mononuclear cells and flow cytometry

Monocyte isolation from whole blood and flow cytometry were performed as described before [21].

Transfection of CHO cells and adenoviral infection of endothelial cells

All transfections of CHO-K1 cells were performed at passage 2 using standard electroporation protocols. Cells were grown to a density of 80% and approximately 20–60 μg DNA was used for 1×10^7 cells. On the following day, cells were subject to selection. Once single cell clones became visible, cells were washed every second to third day with PBS and remaining cells were cultured until 70–80% confluence. Cells were then harvested and after limited dilution, single cells were allowed to grow to colonies in six-well plates. The colonies derived from single cell clones only were analysed for expression of transfected receptors by flow cytometry.

HUVECs and HMECs were transfected with an adenoviral system obtained from ProCorde (Munich, Germany) using a pTR-UF5 plasmid containing CD7/VCAM-1. After washing with PBS, cells were incubated with 1×10^9 pfu per well for 2 hrs. Expression was verified by flow cytometry 48 hrs after the transfection using FITC labeled anti-CD7 antibody.

Adhesion assays

For inhibition studies of cell adhesion, 96-well plates were coated overnight at 4°C with 30 μg/ml fibrinogen. After blocking with 1% BSA, 2×10^4 cells per well were plated and incubated for 2 hrs at 37°C. After incubation, the supernatant was removed, adherent cells were trypsinized, and collected into the appropriate tubes. Samples were stained with a FITC-labeled anti-CD7 antibody and analyzed by flow cytometry. 96-well plates were coated with 20 μg/ml fibrinogen overnight at 4°C and blocked with 1% BSA. 1×10^6 cells/ml were allowed to adhere for 1 hr at 37°C. After washing with PBS, cells were incubated with 50 μl (6 mg/ml) phosphatase substrate (Sigma-Aldrich, St. Louis, MO, USA) for 1 hr at 37°C and the generated p-Nitro phenyl phosphate was measured at 405 nm after the reaction was stopped with 50 μl 1-M. NaOH. Monocyte adhesion assays were performed on a confluent cell layer to avoid attachment of monocytes to the plastic, according to a previously published method [22]. Cells were washed with PBS and co-incubated for 60 min. with monocytes suspended in medium to a density of 2×10^6 (0.5 ml/well). Monocyte suspension was withdrawn and the wells were washed twice with PBS to remove non-adherent cells. Cells and cell aggregates were detached by mild trypsinization, washed by centrifugation (8 min. at $200 \times g$), stained with anti-CD45-FITC and anti-CD14-PE, fixed and analysed (10,000 cells per sample) by flow cytometry. The proportion of monocytes in the suspension was evaluated by the relationship between CD45-FITC and CD14-PE. The absolute number of monocytes adhering to endothelial cells was calculated in relation to the total number of cells obtained after trypsinization. The results were expressed as a percentage of monocytes added.

Monocyte chemotaxis assay

HUVECs were grown on the bottom of the inlets of a 24-well chemotaxis transwell plate (5 μm, Polycarbonate-Membrane, Fisher Scientific, Schwerte, Germany), until confluent. Monocyte suspension (0.2 ml of 10^6 cells/ml) was plated on the upper chamber. The lower chamber was filled with 50 ng/ml MCP-1 medium. After 3 hrs of incubation, the migrated cells on the lower surface of the membrane were fixed, stained with Wright's color (Sigma-Aldrich, St. Louis, MO, USA) and the number of migrated cells per field was counted with an inverted phase-contrast microscope (Nikon, Tokyo, Japan). Six fields were selected in each experiment, and substituted for the average value of counting as an index of migration.

Immunofluorescence

Glass cover slips (12 mm circular, No. 1; Nunc, Rochester, NY, USA) were incubated with fibrinogen (30 μg/ml) at 4°C overnight. After washing with PBS, the cover slips were blocked with 1% BSA and washed twice again with PBS. 1×10^6 cells were allowed to adhere on the coated cover slips for 60 min. at 37°C. Cells were then washed again and fixed with 1% paraformaldehyde/1% Triton X100 for 10 min. at 4°C. For microscopy, cells were stained with an anti-CD7 antibody for 30 min., then washed twice again and stained with a FITC-labeled goat anti-mouse IgG+M antibody and phalloidin-TRITC for 30 min. After another two washes with PBS, cover slips were mounted using Vectashield (Vector, Burlingame, CA, USA). Photographs were taken on an Axioplan-2 microscope (Zeiss, Jena, Germany).

Flow chamber assay

Monocyte adhesion to confluent monolayers of activated (TNF-α 100 ng/ml or IL-1β 166 ng/ml for 12 hrs, Roche, Penzberg, Germany) or non-activated HMECs was investigated using a parallel plate flow chamber (GlycoTech, Gaithersburg, MD, USA). Cells were grown on a 35-mm dish (Nunc, Rochester, NY, USA), which formed the bottom of the parallel plate flow chamber. The chamber and the tubing leading to and from the chamber were filled with buffer, before Calcein AM labeled monocytes (10^6 cells/ml) resuspended in PBS (Invitrogen, Carlsbad, CA, USA) were allowed to flow over HMECs. A defined shear rate of 0.5 dyne/cm^2 was applied with a perfusion pump (Syringe pump phd2000 system, Harvard apparatus, Holliston, MA, USA). Monocyte interaction with the endothelial monolayer was visualized by video microscopy using 20× magnification (Zeiss Axioplan II, Jena, Germany). Cell rolling was assessed in randomly selected 5 sec. video frames and cell adhesion was counted in randomly selected optical fields (mean ± S.D. of 6 randomly chosen fields evaluated). All analyses were performed offline with Let's edit software (Canopus, Kobe, Japan).

Statistical analysis

Data are shown as mean ± S.D.. Quantification of data was evaluated by analysis of variance (ANOVA). *Post-hoc* Tukey analysis was used to compare differences between groups (*$P < 0.1$; **$P < 0.01$; ***$P < 0.001$). All statistical analyses were performed with the Prism software package Version 4 (GraphPad Software, La Jolla, CA, USA).

Results

We used a glycoprotein receptor $\alpha_{IIb}\beta_3$-based CHO cell model system to assess the influence of the transfection of different CD7/β_3 chimeras on cytoskeletal anchorage and $\alpha_{IIb}\beta_3$-mediated cell adhesion. We then constructed a CD7/VCAM-1 chimera corresponding to the CD7/β_3 construct that had the strongest inhibitory effect on cytoskeletal anchorage and adhesion (Fig. 1). This CD7/VCAM-1 chimera was used to interfere with native VCAM-1 in a dominant negative manner.

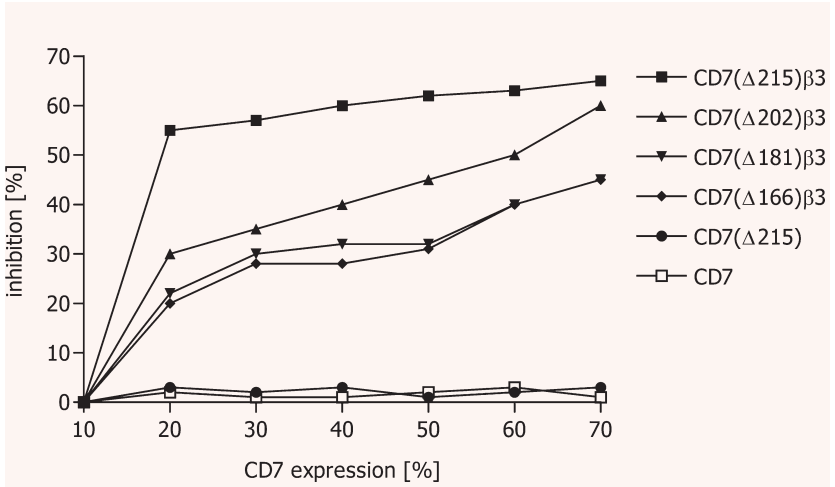

Fig. 2 Inhibition of cell adhesion of transfected CHO cells on immobilized fibrinogen. Cells were transfected with different CD7/β_3 constructs and treated with different concentrations of doxycycline to regulate the CD7/β_3 expression level, which was measured by flow cytometry using a fluorescein-conjugated anti-CD7 antibody. Cell adhesion was determined by quantitative flow cytometry of cells in the supernatant and after trypsin treatment. The fusion-construct CD7(Δ215)β_3 resulted in strong inhibition of cell adhesion at low levels of expression, consistent with a dominant negative inhibition. The other fusion constructs resulted in inhibition that is dependent on the level of expression, indicating competitive inhibition.

Construction of CD7/β_3 fusion proteins

We designed four CD7/β_3 fusion proteins with differing fusion sites between the N-terminal CD7 and the C-terminal β_3 as well as a truncated CD7 control construct (Fig. 1). First, we investigated how these CD7/β_3 constructs affect the cytoskeletal anchorage of the native $\alpha_{IIb}\beta_3$ receptor. We used the Tet Off^{TM}-System in order to achieve different expression levels of the constructs by the addition of various levels of tetracycline. Comparing the different CD7/β_3 constructs and different expression levels (100% of expression was observed in the absence of tetracycline) we found that a low membrane expression of the fusion protein CD7(Δ215)β_3 is sufficient to achieve a significant blockade of $\alpha_{IIb}\beta_3$-mediated adhesion *via* a dominant negative inhibition mechanism. Moving the fusion site between CD7 and β_3 towards the cell membrane and having the intracellular domain of β_3 at its correct orientation/distance, in respect to the cell membrane and the cytoskeletal anchorage structures, switched the dominant negative inhibition of CD7(Δ215)β_3 to competitive inhibition of the other CD7/β_3-fusion constructs (Fig. 2). This was confirmed in adhesion assays (data not shown). Because of its advantageous dominant negative inhibition, the fusion protein CD7(Δ215)β_3 was chosen for further functional assays.

CD7(Δ215)β_3 inhibits $\alpha_{IIb}\beta_3$-mediated adhesion to fibrinogen, adhesion plaque formation and actin stress fibre formation

We transfected the native $\alpha_{IIb}\beta_3$ receptor into CHO cells either alone or in combination with the CD7(Δ215)β_3 and tested the cells for their ability to adhere to fibrinogen. In contrast to wild-type CHO cells, which are unable to spread on fibrinogen, $\alpha_{IIb}\beta_3$-expressing CHO cells firmly adhered and spread on this surface (Fig. 3A). When stained with anti-α_{IIb} and phalloidin-TRITC, these cells exhibited strong focal adhesion plaques and actin stress fibre formation. After transfection with CD7(Δ215)β_3, the cells did not spread and were mainly round in shape. Staining with anti-α_{IIb} revealed a lack in adhesion plaque formation; furthermore, phalloidin-TRITC staining revealed no actin stress fibre formation. Overall, cell adhesion was significantly reduced by CD7(Δ215)β_3 (Fig. 3B), confirming the dominant negative inhibitory effect of this construct. This was not observed in cells transfected with CD7(Δ215) lacking the intracellular β_3 part (data not shown). The binding of $\alpha_{IIb}\beta_3$-expressing CHO cells to fibrinogen was significantly reduced by the $\alpha_{IIb}\beta_3$-function blocking antibody ReoPro (abciximab, 10 μg/ml) demonstrating the specificity of our CHO cell system for $\alpha_{IIb}\beta_3$-mediated adhesion (Fig. 3C).

Inhibition of monocyte adhesion to VCAM-1 expressing CHO cells by CD7/VCAM-1

Based on the results obtained with the CD7(Δ215)β_3 chimera exhibiting strong dominant negative inhibition, we constructed a CD7/VCAM-1 chimera utilizing the same approach with a spatial separation of the VCAM-1 intracellular domain from the cell membrane (Fig. 1). First, we evaluated the impact of CD7/VCAM-1 transfection on VCAM-1-expressing CHO cells in regard to monocyte adhesion. Using again the Tet Off^{TM}-system, we were able to modulate the expression of the CD7/VCAM-1 chimera. Double transfected (CD7/VCAM-1 and VCAM-1) cells treated with doxycycline, down regulating CD7/VCAM-1 expression, showed similar monocyte adhesion when compared to VCAM-1-expressing CHO cells. In contrast, double transfected (CD7/VCAM-1 and VCAM-1) CHO cells without doxycycline treatment showed significantly less monocyte adhesion (Fig. 4A). Thus, CD7/VCAM-1 co-expression was able to inhibit VCAM-1-mediated monocyte adhesion.

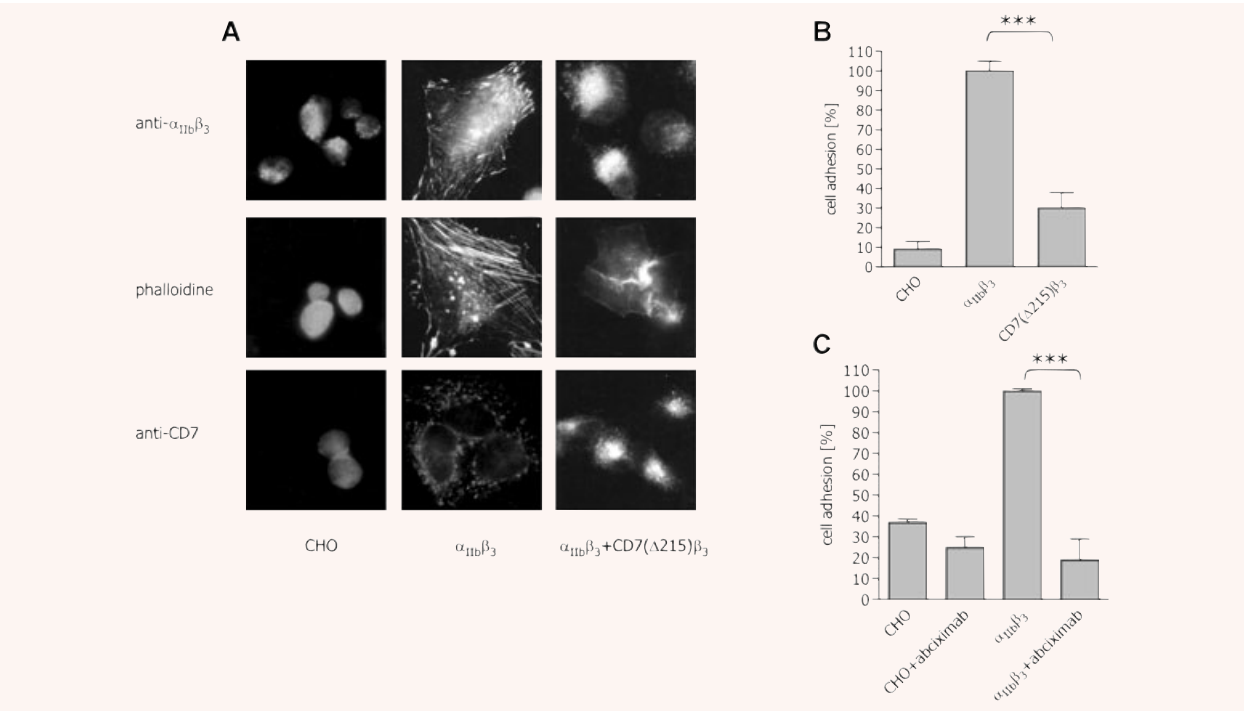

Fig. 3 Loss of cytoskeletal anchorage of $\alpha_{IIb}\beta_3$ upon CD7(Δ215)β_3 transfection. (A) Cells were transfected with $\alpha_{IIb}\beta_3$ and $\alpha_{IIb}\beta_3$ + CD7(Δ215)β_3. Staining was performed with anti-$\alpha_{IIb}\beta_3$-FITC, anti-phalloidin-TRITC and anti-CD7-FITC. $\alpha_{IIb}\beta_3$-expressing cells adhere and spread on fibrinogen and the interaction between integrin and cytoskeleton is manifested by the localization of $\alpha_{IIb}\beta_3$ in adhesion plaques and the organization of the actin cytoskeleton in stress fibres that span between adhesion plaques. After co-transfection with CD7(Δ215)β_3 $\alpha_{IIb}\beta_3$-expressing cells do not form adhesion plaques and do not form stress fibres. (B) Quantification of cell adhesion of transfected CHO cells on fibrinogen. Cells were transfected with $\alpha_{IIb}\beta_3$ and $\alpha_{IIb}\beta_3$ + CD7(Δ215)β_3. Adhesion of $\alpha_{IIb}\beta_3$-transfected CHO cells were set to 100% adhesion. Binding was significantly reduced by co-transfection with CD7 (Δ215)β_3. Mean ± S.D. for $n = 6$ are given (***$P < 0.001$). (C) Quantification of cell adhesion of $\alpha_{IIb}\beta_3$-expressing CHO cells on fibrinogen under the influence of ReoPro (abciximab, 10 μg/ml). Adhesion of $\alpha_{IIb}\beta_3$-transfected CHO cells was set to 100% adhesion. Binding was significantly reduced by ReoPro. Mean ± S.D. for $n = 3$ are given (***$P < 0.001$).

To further characterize the VCAM-1 monocyte interaction, we studied the effect of anti-VCAM-1 and anti-VLA-4 (CD49d/CD29) (both 10 μg/ml for 15 min.) antibody treatment. After pre-incubation with anti-VCAM-1, the amount of adhering monocytes to double transfected (CD7/VCAM-1 and VCAM-1) CHO cells was reduced to control levels (Fig. 4B). We observed comparable results by blocking the VCAM-1 counter receptor VLA-4 on monocytes using an anti-CD49d antibody (Fig. 4C). Furthermore, we used cytochalasin D, an inhibitor of actin polymerization to interrupt the cytoskeletal organization. After doxycycline treatment (to suppress expression of CD7/VCAM-1), cytochalasin D reduced monocyte binding significantly ($P < 0.001$) (Fig. 4A). This indicates that cytoskeletal anchorage is necessary for the proper function of VCAM-1 and that CD7/VCAM-1 competes with VCAM-1 in its interaction with the actin cytoskeleton.

The specificity of the CD7/VCAM-1 construct to inhibit VCAM-1 was assessed in CHO cells stably expressing either ICAM-1 or E-selectin. We found no effect of CD7/VCAM-1 transfection on ICAM-1-mediated monocyte adhesion, but treatment with cytochalasin D (Fig. 4D) as well as pre-incubation with a function blocking anti-ICAM-1-antibody (10 μg/ml for 15 min.) significantly reduced monocyte adhesion (Fig. 4E). In addition, monocyte adhesion to CHO cells transfected with E-selectin was also not affected by co-transfection of CD7/VCAM-1, but a function blocking anti-E-selectin-antibody (10 μg/ml for 15 min.) led to a significant reduction in the number of adhering monocytes (Fig. 4F). Treatment with cytochalasin D had no effect on E-selectin mediated monocyte adhesion, indicating monocyte binding to E-selectin is independent of cytoskeleton interaction (Fig. 4G). These results implicate a highly specific action of CD7/VCAM-1 on the native VCAM-1 receptor.

Inhibition of VCAM-1-mediated monocyte transmigration by CD7/VCAM-1

After observing the influence of the CD7/VCAM-1 chimera on monocyte adhesion, we studied the transmigration of monocytes

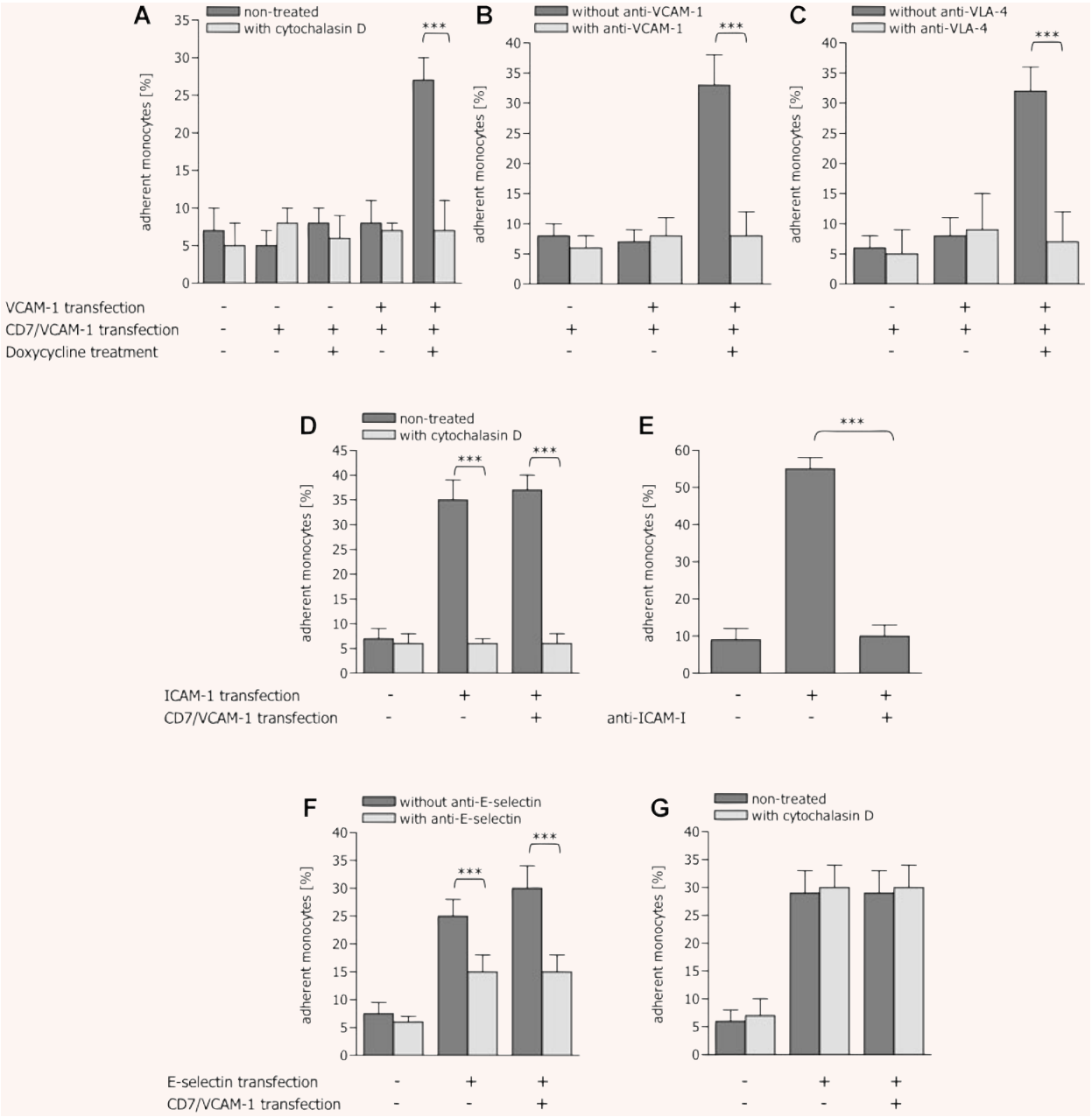

Fig. 4 VCAM-1, ICAM-1 and E-selectin mediated monocyte adhesion after treatment with CD7/VCAM-1, cytochalasin D, anti-VCAM-1, anti-VLA-4 and anti-E-selectin. Cells were transfected with either VCAM-1, ICAM-I, E-selectin, CD7/VCAM-1 or co-transfected. Expression of CD7/VCAM-1 was down regulated by doxycycline treatment. CD7/VCAM-1 effectively inhibits VCAM-1 but not ICAM-1 or E-selectin mediated monocyte adhesion. Adhesion was reduced after cytochalasin D treatment (50 ng/ml for 4 hrs) (A), anti-VCAM-1 (B) as well as anti-VLA-4 incubation (both 10 μg/ml for 15 min.) (C). Adhesion was reduced in ICAM-I transfected cells after cytochalasin D treatment but not after CD7/VCAM-1 co-transfection (D) and after incubation with anti-ICAM-I antibodies (E). Adhesion was reduced in E-selectin transfected cells after incubation with anti-E-selectin antibodies (F), but not after CD7/VCAM-1 co-transfection or cytochalasin D treatment (G). Mean ± S.D. for $n = 6$ are given (***$P < 0.001$).

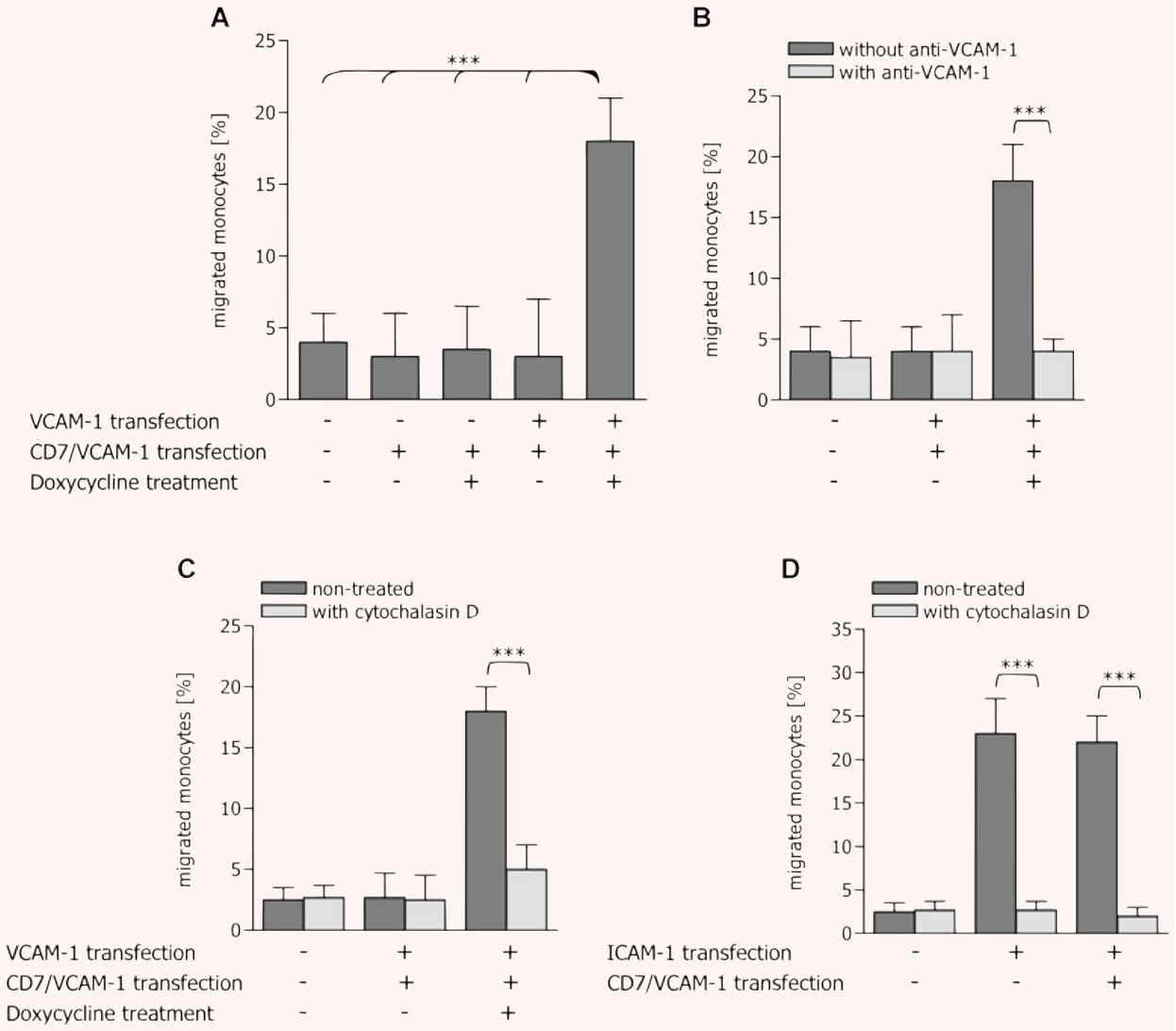

Fig. 5 VCAM-1 and ICAM-1 mediated monocyte migration after treatment with CD7/VCAM-1, cytochalasin D and anti-VCAM-1. Cells were transfected with either VCAM-1, ICAM-I, CD7/VCAM-1 or co-transfected. Expression of CD7/VCAM-1 was down regulated by doxycycline treatment. Monocyte migration through VCAM-1-expressing CHO cells was inhibited by CD7/VCAM-1 (A), anti-VCAM-1 (B) and after cytochalasin D treatment (C). Migration of monocytes through ICAM-1-expressing CHO cells was not inhibited by transfection with CD7/VCAM-1, but cytoskeletal anchorage was essential for ICAM-1-mediated migration (D). Mean ± S.D. for $n = 6$ are given (***$P < 0.001$).

through a cell layer of transfected CHO cells. We measured chemotaxis using a 24-well chemotaxis chamber containing an insert filter with monocytes plated onto the upper chamber. More monocytes were able to migrate through VCAM-1 expressing CHO cells compared with control CHO cells and CHO cells expressing CD7/VCAM-1 (Fig. 5A). Co-expression of CD7/VCAM-1 and VCAM-1 led to a significant reduction of migration to levels observed with the CHO control cells and suppression of CD7/VCAM-1 expression by doxycycline treatment significantly increased monocyte transmigration. Thus, VCAM-1 significantly contributes to monocyte transmigration, which is inhibitable by the newly developed approach targeting the cytoskeletal anchorage of VCAM-1 (Fig. 5A).

Transmigration was further characterized by antibody pre-incubation to block monocyte-to-cell interaction. Anti-VCAM-1 incubated double transfected CHO cells showed less monocyte migration compared to non-treated double transfected cells. Suppression of CD7/VCAM-1 expression restored transmigration,

demonstrating a VCAM-1-mediated migration of monocytes (Fig. 5B). Interruption of cytoskeletal anchorage with cytochalasin D had the same effect as co-transfection of CD7/VCAM-1 (Fig. 5C).

Involvement of ICAM-1 in monocyte transmigration has been reported [23]. Cytochalasin D treatment abolished monocyte migration through ICAM-1 expressing CHO cells, indicating that as well as for VCAM-1 cytoskeletal anchorage is necessary for ICAM-1 function, but CD7/VCAM-1 transfection did not reduce the migration ability of ICAM-1 transfected CHO cells to control levels, providing further evidence of the target specificity of CD7/VCAM-1 (Fig. 5D).

Adenoviral transfer of CD7/VCAM-1 to HUVECs inhibits monocyte adhesion and attenuates monocyte transmigration

Finally, we tested the effect of CD7/VCAM-1 transfection directly in human umbilical vein endothelial cells (HUVEC) and human microvascular endothelial cells (HMEC). With HUVECs, more adherent monocytes were detected with IL-1β stimulated cells compared to non-stimulated HUVECs. IL-1β rapidly up regulates VCAM-1 and E-selection in human endothelial cells (data not shown). Transfection with CD7/VCAM-1 resulted in a significant reduction of adhesion for non-stimulated and stimulated cells (Fig. 6A). Vector-only transfected control cells showed similar levels of adhesion as non-transfected cells. Co-expression of CD7/VCAM-1 reduced the level of monocyte adhesion from inflammatory levels to non-inflammatory levels (Fig. 6A). Non-stimulated HUVECs and CD7/VCAM-1 transfected HUVECs showed no difference in VCAM-1-mediated transmigration. After stimulation with IL-1β, the migration level was significantly enhanced in non-transfected as well as mock-transfected cells. CD7/ VCAM-1 transfection significantly reduced the migration of monocytes (Fig. 6B).

Adenoviral transfer of CD7/VCAM-1 to an endothelial cell (HMEC) monolayer reduced rolling and adhesion of monocytes under shear stress

In a flow chamber system, stimulation of HMECs with IL-1β significantly increased the number of adherent monocytes. Although a smaller but nevertheless a significant increase in the number of rolling monocytes was seen. Transfection with CD7/VCAM-1, incubation with anti-VCAM-1 antibodies and the combination of both resulted in a significant reduction of monocyte adhesion, reflecting the crucial role of VCAM-1 for stable adhesion. The impact on monocyte rolling was less obvious, indicating a minor role for VCAM-1 in mediating monocyte rolling (Fig. 6C compared to 6D). However, following IL-1β stimulation, CD7/VCAM-1 transfection also significantly inhibited monocyte rolling.

Discussion

Local treatment of rupture-prone atherosclerotic plaques and prevention of atherosclerosis are major challenges in cardiovascular medicine. Adhesion receptors play a crucial role in the development of atherosclerosis by mediating the required cell–cell interactions leading to the establishment of atherosclerotic plaques. Cytoskeletal anchorage is necessary for the function of many adhesion receptors including the integrin $\alpha_{IIb}\beta_3$, for which proper anchorage is a prerequisite for its multiple functions [13, 16]. The integrin cytoplasmic tails in general and the cytoplasmic domain of the integrin β-subunits in particular are crucial for the interaction with the cell's cytoskeleton. The interruption of integrin β-subunits' cytoskeletal anchorage results in the loss of adhesive function [20, 24]. Therefore, we postulated that β_3-chimeras, with an inert extracellular component, may compete with the native receptors' cytoskeletal anchorage, thereby interfering with receptor clustering, signaling and adhesive properties of the receptor. Our concept of competitive and potentially dominant negative inhibition of cytoskeletal anchorage was first established in an integrin $\alpha_{IIb}\beta_3$-based CHO cell model (Figs 2 and 3).

The extracellular part of CD7, a small membrane protein (40 kD) of the Ig-superfamily [25] was used for the construction of CD7/β_3-chimeras as it is generally considered as an inert extracellular marker. CD7 is found on mature T cells, natural killer cells [26, 27] and on B-cells or myeloid precursor cells before they enter the thymus during embryonic development [28, 29]. It is also used as a diagnostic marker for lymphatic T cell leukemia [30] and has recently been used for the targeting of soluble Fas-Ligand (sFasL) to CD7-expressing cells *via* a CD7 specific single-chain antibody as a novel therapeutic approach for acute T cell leukemia [31]. Depending on the fusion site between CD7 and β_3 two mechanism of inhibition seem to occur in our CHO cell model (Figs 1 and 2). The construct CD7(Δ215)β_3 (Fig. 1) caused a dominant negative inhibition whereas the other fusion constructs caused a competitive inhibition of integrin $\alpha_{IIb}\beta_3$-mediated adhesion.

Dominant negative inhibition achieved with integrin β-subunit-chimeras has been linked to competition of the β-subunit cytoplasmic tails for talin binding [32]. However, it has recently been shown that talin alone does not fully account for the dominant negative inhibition observed by co-expression of integrin β-subunit-chimeras [33]. Furthermore, the same group proposed that unique structural changes in the integrin cytoplasmic tail associated with the chimerization account for the non-talin mediated effects on the integrin–cytoskeletal linkage of the native receptor. In addition, the fusion site in our CD7(Δ215)/β_3 construct results in spatial separation of the β_3 cytoplasmic domain from the cell membrane, which may cause the disruption of large focal adhesion complexes. This may explain our finding that only a few constructs led to the major impairment in $\alpha_{IIb}\beta_3$-mediated adhesion, constituting a dominant negative inhibitory effect.

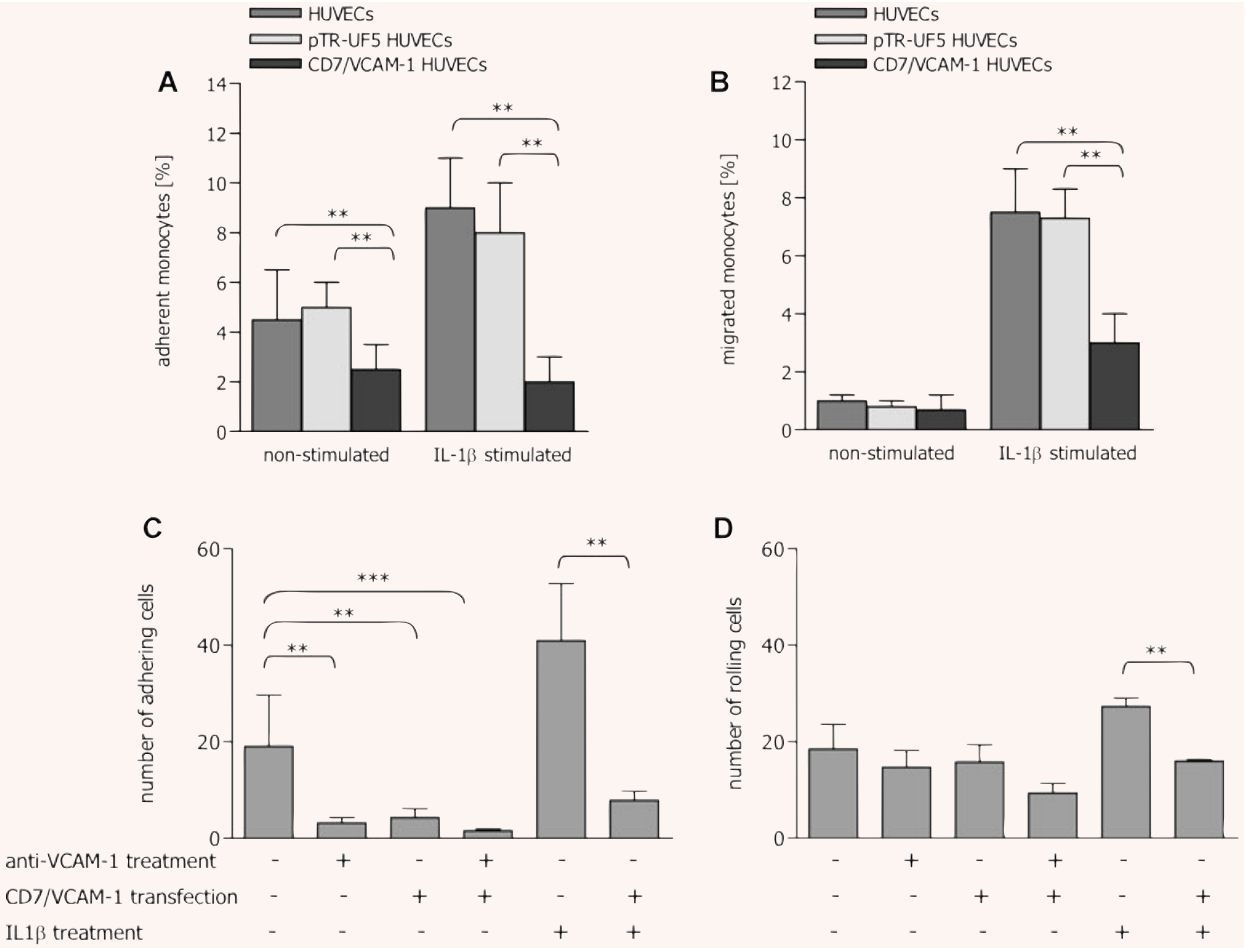

Fig. 6 Monocytes adhesion, migration and rolling are inhibited by CD7/VCAM-1. Cells were incubated with buffer (non-stimulated) or stimulated with IL-1β (IL-1β-stimulated) and transfected with the vector alone (pTR-UF5 HUVECs) or the CD7/VCAM-1 fusion protein (CD7/VCAM-1 HUVECs). After IL-1β stimulation, monocyte adhesion and migration increased. (A) Adhesion could be significantly reduced after CD7/VCAM-1 transfection in non-stimulated and stimulated HUVECs. (B) For cell migration, cell activation is a prerequisite. On stimulated HUVECs, monocyte migration could be inhibited by the CD7/VCAM-1 fusion protein. Mean ± S.D. for $n = 6$ are given (**$P < 0.01$). HMECs in a flow chamber assay were stimulated with buffer or IL-1β and transfected with CD7/VCAM-1 fusion protein and/or blocked with an anti-VCAM-1 antibody (10 μg/ml for 15 min.). Increased amounts of adherent (C) and rolling monocytes (D) are detected after IL-1β stimulation. Transfection with CD7/VCAM-1, incubation with anti-VCAM-1 antibodies, and the combination of both result in a reduction of monocyte adhesion and rolling. Mean ± S.D. for $n = 6$ are given (**$P < 0.01$; ***$P < 0.001$).

The CD7/VCAM-1 chimera was designed on the blueprints of the CD7(−Δ215)/β_3 construct composed of the CD7 extracellular domain, transmembrane domain, and parts of the intracellular domain fused to the VCAM-1 cytoplasmic domain spatially separated from the cell membrane. Its purpose was to target the adhesive function on endothelial cells towards its counter receptor VLA-4 on monocytes by altering the cytoskeletal anchorage of VCAM-1.

The blockade of VCAM-1 appears to be a promising approach to reduce vascular damage [34]. There is strong evidence that VCAM-1 is one of the major players in monocyte recruitment [8, 35] and it has been shown to enhance monocyte and macrophage adhesion in rats [36], mice [37] and rabbits [38]. Furthermore, blockade of VCAM-1 with monoclonal antibodies has been shown to inhibit adhesion and transmigration of a human monocyte cell line to human aortic endothelial cells [39]. Anti-oxidative drugs have been found to repress ICAM-1 and VCAM-1 [40]. Direct blockade of the VCAM-1 counter receptor VLA-4 with different specific peptides has been observed to successfully attenuate monocyte migration and inflammatory

reactions [41]. Blockade of VCAM-1 in hypercholesterolaemic mice has been shown to result in reduced neointima formation due to the inhibition of monocyte migration [42, 43]. Gene targeting experiments highlighting the importance of VLA-4 and VCAM-1 in atherosclerotic lesion development have been hampered by the lack of availability of appropriate knockout mice. Mice with a homozygote deficiency in the fourth domain of VCAM-1, which binds VLA-4, have been shown to survive and to have reduced monocyte binding and an 84% reduction in lesions in the aortic root when crossed with ApoE–/– knockout mice [35]. However, null mutations for VCAM-1 lead to embryonic lethality [44] such that no adult mice are available to study the impact of these molecules on atherosclerosis.

All approaches that aim for systemic targeting of VCAM-1 may lead to unwanted side effects, due to the inhibition of physiological VCAM-1 functions in healthy tissues. Therefore, an ongoing effort continues into the development of agents that allow for the regional blockade of VCAM-1. Knockdown of VCAM-1 expressed on activated vascular endothelium has been achieved by siRNA transfection in mice. However, significant up regulation of other adhesion molecules associated with cell stress occurred after siRNA transfection [45]. Cell-specific and inducible strategies have been developed that appear to be able to eliminate VCAM-1 in certain cell types only [46, 47].

Our gene therapy approach is based on targeting of VCAM-1 *via* a CD7/VCAM-1 fusion protein using an adenoviral vector system that would allow local application. Transfection of the CD7/VCAM-1 construct as an inert competitor to wild-type VCAM-1 in stably transfected CHO cells blocked VCAM-1 mediated monocyte adhesion (Fig. 4A–C) and migration (Fig. 5A–C) to the same extent as achieved by antibody blockade of VCAM-1. This indicates that CD7/VCAM-1 causes a dominant negative inhibition of VCAM-1 similar to the dominant negative inhibition of $\alpha_{IIb}\beta_3$, which we observed with the initial CD7/β_3 construct (Figs 2 and 3). Furthermore, our data underline the importance of VCAM-1 in mediating monocyte adhesion and migration in our CHO cell system without co-expression of, or interaction with, other surface receptors. However, because *in vivo* E-selectin, ICAM-1 and VCAM-1 are all expressed in parallel under inflammatory conditions we investigated their role separately in our CHO-cell based experimental system. In agreement with others [48], our studies confirm that E-selectin alone can also mediate monocyte adhesion but not migration (Fig. 4F–G), whereas ICAM-1 is able to mediate both adhesion (Fig. 4D–E) and migration (Fig. 5D). Furthermore co-transfection with CD7/VCAM-1 had no impact on ICAM-1 or E-selectin mediated monocyte adhesion therefore indicating that the dominant negative inhibition of our CD7/VCAM-1 construct is highly specific for VCAM-1.

For E-selectin, this finding was less surprising as cytoskeletal anchorage is not necessary for this molecule. For ICAM-1, however, one could suggest a similar binding site as for VCAM-1. Earlier reports have demonstrated α-actin association [49] for ICAM-1. Using cytochalasin D as an inhibitor of actin stress fibre formation, we found, in agreement with others, that the association of ICAM-1 with actin-containing structures of the cytoskeleton is necessary for proper function [50] (Figs 4D and 5D), whereas monocyte adhesion mediated by E-selectin occurs without cytoskeletal anchorage [51] (Fig. 4G). We also found that cytochalasin D blocked VCAM-1-mediated monocyte adhesion and migration to the same level as seen with CD7/VCAM-1 transfection (Figs 4A and 5C), strongly supporting our hypothesis that cytoskeletal anchorage is necessary for the proper function of VCAM-1. Our data suggest different interaction sites for VCAM-1 and ICAM-1 with the cytoskeleton, which needs further exploration in future studies.

Finally, we examined monocyte adhesion under conditions of shear stress after adenoviral delivery of our construct to primary and immortalized human endothelial cells (HUVECs and HMECs). Our CD7/VCAM-1 construct significantly inhibited VCAM-1-mediated adhesion and migration of human monocytes (Fig. 6) in these cells. The extent of inhibition achieved with our gene therapy approach is similar to earlier reported studies, in which anti-VCAM-1 antibodies were used to block lateral monocyte migration and transendothelial migration mediated by the interaction of VLA-4 and VCAM-1 [52]. Our findings indicate that adenoviral-mediated transfer of the CD7/VCAM-1 construct is feasible and results in dominant negative inhibition of VCAM-1-mediated function, leading to significantly reduced endothelial monocyte adhesion and transmigration. The proposed anti-atherosclerotic action of adenoviral-mediated local CD7/VCAM-1 transfection will be explored in further studies using an animal model of atherosclerosis.

In conclusion, our study confirms the crucial role of VCAM-1 in adhesion, accumulation and migration of monocytes. Our findings strengthen the rationale for the development of therapies aimed at inhibiting the interaction between VLA-4 on monocytes and VCAM-1 on activated endothelial cells. To our knowledge, this is the first description of a blockade of this interaction *via* co-expression of a competing CD7/VCAM-1 fusion protein interfering with the cytoskeletal anchorage of VCAM-1. Based on a dominant negative inhibitory effect, the described gene therapeutic approach promises a regional, localized blockade of VCAM-1 function *via* the local delivery of only a small number of CD7/VCAM-1 constructs. This unique approach might allow a localized treatment of atherosclerosis.

Acknowledgements

N.B., K.P. and C.E.H. are supported by the National Health and Medical Research Council of Australia. K.P. is supported by the Heart Foundation of Australia. C.E.H. and I.A. are supported by the Deutsche Forschungsgemeinschaft (DFG Ha 5297/1-1 & Ah 185/1-1, respectively). We thank Drs. S. Marheineke and J. Lee for technical support and Drs. A. Straub and B. Smith for critical reading of the manuscript.

References

1. **Libby P.** Inflammation in atherosclerosis. *Nature*. 2002; 420: 868–74.
2. **Swirski FK, Pittet MJ, Kircher MF, *et al.*** Monocyte accumulation in mouse atherogenesis is progressive and proportional to extent of disease. *Proc Natl Acad Sci USA*. 2006; 103: 10340–5.
3. **Gawaz M, Langer H, May AE.** Platelets in inflammation and atherogenesis. *J Clin Invest*. 2005; 115: 3378–84.
4. **Cybulsky MI, Fries JW, Williams AJ, *et al.*** Alternative splicing of human VCAM-1 in activated vascular endothelium. *Am J Pathol*. 1991; 138: 815–20.
5. **O'Brien KD, Allen MD, McDonald TO, *et al.*** Vascular cell adhesion molecule-1 is expressed in human coronary atherosclerotic plaques. Implications for the mode of progression of advanced coronary atherosclerosis. *J Clin Invest*. 1993; 92: 945–51.
6. **Pei H, Wang Y, Miyoshi T, *et al.*** Direct evidence for a crucial role of the arterial wall in control of atherosclerosis susceptibility. *Circulation*. 2006; 114: 2382–9.
7. **Iiyama K, Hajra L, Iiyama M, *et al.*** Patterns of vascular cell adhesion molecule-1 and intercellular adhesion molecule-1 expression in rabbit and mouse atherosclerotic lesions and at sites predisposed to lesion formation. *Circ Res*. 1999; 85: 199–207.
8. **Kawakami A, Aikawa M, Alcaide P, *et al.*** Apolipoprotein CIII induces expression of vascular cell adhesion molecule-1 in vascular endothelial cells and increases adhesion of monocytic cells. *Circulation*. 2006; 114: 681–7.
9. **Nahrendorf M, Jaffer FA, Kelly KA, *et al.*** Noninvasive vascular cell adhesion molecule-1 imaging identifies inflammatory activation of cells in atherosclerosis. *Circulation*. 2006; 114: 1504–11.
10. **Broisat A, Riou LM, Ardisson V, *et al.*** Molecular imaging of vascular cell adhesion molecule-1 expression in experimental atherosclerotic plaques with radiolabelled B2702-p. *Eur J Nucl Med Mol Imaging*. 2007; 34: 830–40.
11. **Hordijk PL.** Endothelial signalling events during leukocyte transmigration. *Febs J*. 2006; 273: 4408–15.
12. **Arnaout MA, Mahalingam B, Xiong JP.** Integrin structure, allostery, and bidirectional signaling. *Annu Rev Cell Dev Biol*. 2005; 21: 381–410.
13. **Peter K, Ahrens I, Schwarz M, *et al.*** Distinct roles of ligand affinity and cytoskeletal anchorage in alphaIIb-beta3 (GP IIb/IIIa)-mediated cell aggregation and adhesion. *Platelets*. 2004; 15: 427–38.
14. **Peter K, Bode C.** A deletion in the alpha subunit locks platelet integrin alpha IIb beta 3 into a high affinity state. *Blood Coagul Fibrinolysis*. 1996; 7: 233–6.
15. **O'Toole TE, Katagiri Y, Faull RJ, *et al.*** Integrin cytoplasmic domains mediate inside-out signal transduction. *J Cell Biol*. 1994; 124: 1047–59.
16. **Ahrens IG, Moran N, Aylward K, *et al.*** Evidence for a differential functional regulation of the two beta(3)-integrins alpha(V)beta(3) and alpha(IIb)-beta(3). *Exp Cell Res*. 2006; 312: 925–37.
17. **Morishige K, Shimokawa H, Yamawaki T, *et al.*** Local adenovirus-mediated transfer of C-type natriuretic peptide suppresses vascular remodeling in porcine coronary arteries *in vivo*. *J Am Coll Cardiol*. 2000; 35: 1040–7.
18. **Deiner C, Schwimmbeck PL, Koehler IS, *et al.*** Adventitial VEGF165 gene transfer prevents lumen loss through induction of positive arterial remodeling after PTCA in porcine coronary arteries. *Atherosclerosis*. 2006; 189: 123–32.
19. **Fishbein I, Alferiev I, Bakay M, *et al.*** Local delivery of gene vectors from bare-metal stents by use of a biodegradable synthetic complex inhibits in-stent restenosis in rat carotid arteries. *Circulation*. 2008; 117: 2096–103.
20. **Peter K, O'Toole TE.** Modulation of cell adhesion by changes in alpha L beta 2 (LFA-1, CD11a/CD18) cytoplasmic domain/cytoskeleton interaction. *J Exp Med*. 1995; 181: 315–26.
21. **Eisenhardt SU, Schwarz M, Schallner N, *et al.*** Generation of activation-specific human anti-alphaMbeta2 single-chain antibodies as potential diagnostic tools and therapeutic agents. *Blood*. 2007; 109: 3521–8.
22. **Zapolska-Downar D, Naruszewicz M, Zapolski-Downar A, *et al.*** Ibuprofen inhibits adhesiveness of monocytes to endothelium and reduces cellular oxidative stress in smokers and non-smokers. *Eur J ClinInvest*. 2000; 30: 1002–10.
23. **Languino LR, Duperray A, Joganic KJ, *et al.*** Regulation of leukocyte-endothelium interaction and leukocyte transendothelial migration by intercellular adhesion molecule 1-fibrinogen recognition. *Proc Natl Acad Sci USA*. 1995; 92: 1505–9.
24. **Wiesner S, Legate KR, Fassler R.** Integrin-actin interactions. *Cell Mol Life Sci*. 2005; 62: 1081–99.
25. **Eisenbarth GS, Haynes BF, Schroer JA, *et al.*** Production of monoclonal antibodies reacting with peripheral blood mononuclear cell surface differentiation antigens. *J Immunol*. 1980; 124: 1237–44.
26. **Barcena A, Muench MO, Galy AH, *et al.*** Phenotypic and functional analysis of T-cell precursors in the human fetal liver and thymus: CD7 expression in the early stages of T- and myeloid-cell development. *Blood*. 1993; 82: 3401–14.
27. **Rabinowich H, Pricop L, Herberman RB, *et al.*** Expression and function of CD7 molecule on human natural killer cells. *J Immunol*. 1994; 152: 517–26.
28. **Haynes BF, Mann DL, Hemler ME, *et al.*** Characterization of a monoclonal antibody that defines an immunoregulatory T cell subset for immunoglobulin synthesis in humans. *Proc Natl Acad Sci USA*. 1980; 77: 2914–8.
29. **Vodinelich L, Tax W, Bai Y, *et al.*** A monoclonal antibody (WT1) for detecting leukemias of T-cell precursors (T-ALL). *Blood*. 1983; 62: 1108–13.
30. **Haynes BF, Metzgar RS, Minna JD, *et al.*** Phenotypic characterization of cutaneous T-cell lymphoma. Use of monoclonal antibodies to compare with other malignant T cells. *N Engl J Med*. 1981; 304: 1319–23.
31. **Bremer E, ten Cate B, Samplonius DF, *et al.*** CD7-restricted activation of Fas-mediated apoptosis: a novel therapeutic approach for acute T-cell leukemia. *Blood*. 2006; 107: 2863–70.
32. **Calderwood DA, Tai V, Di Paolo G, *et al.*** Competition for talin results in trans-dominant inhibition of integrin activation. *J Biol Chem*. 2004; 279: 28889–95.
33. **Tanentzapf G, Martin-Bermudo MD, Hicks MS, *et al.*** Multiple factors contribute to integrin-talin interactions *in vivo*. *J Cell Sci*. 2006; 119: 1632–44.
34. **Yusuf-Makagiansar H, Anderson ME, Yakovleva TV, *et al.*** Inhibition of LFA-1/ICAM-1 and VLA-4/VCAM-1 as a therapeutic approach to inflammation and autoimmune diseases. *Med Res Rev*. 2002; 22: 146–67.
35. **Dansky HM, Barlow CB, Lominska C, *et al.*** Adhesion of monocytes to arterial endothelium and initiation of atherosclerosis

are critically dependent on vascular cell adhesion molecule-1 gene dosage. *Arterioscler Thromb Vasc Biol*. 2001; 21: 1662–7.

36. **Landry DB, Couper LL, Bryant SR, *et al.*** Activation of the NF-kappa B and I kappa B system in smooth muscle cells after rat arterial injury. Induction of vascular cell adhesion molecule-1 and monocyte chemoattractant protein-1. *Am J Pathol*. 1997; 151: 1085–95.
37. **Huo Y, Hafezi-Moghadam A, Ley K.** Role of vascular cell adhesion molecule-1 and fibronectin connecting segment-1 in monocyte rolling and adhesion on early atherosclerotic lesions. *Circ Res*. 2000; 87: 153–9.
38. **Gerszten RE, Lim YC, Ding HT, *et al.*** Adhesion of monocytes to vascular cell adhesion molecule-1-transduced human endothelial cells: implications for atherogenesis. *Circ Res*. 1998; 82: 871–8.
39. **Piga R, Naito Y, Kokura S, *et al.*** Short-term high glucose exposure induces monocyte-endothelial cells adhesion and transmigration by increasing VCAM-1 and MCP-1 expression in human aortic endothelial cells. *Atherosclerosis*. 2007; 193: 328–34.
40. **Cominacini L, Garbin U, Pasini AF, *et al.*** Antioxidants inhibit the expression of intercellular cell adhesion molecule-1 and vascular cell adhesion molecule-1 induced by oxidized LDL on human umbilical vein endothelial cells. *Free Radic Biol Med*. 1997; 22: 117–27.
41. **Haworth D, Rees A, Alcock PJ, *et al.*** Anti-inflammatory activity of c(ILDV-NH(CH2)5CO), a novel, selective, cyclic peptide inhibitor of VLA-4-mediated cell adhesion. *Br J Pharmacol*. 1999; 126: 1751–60.
42. **Slepian MJ, Massia SP, Dehdashti B, *et al.*** Beta3-integrins rather than beta1-integrins dominate integrin-matrix interactions involved in postinjury smooth muscle cell migration. *Circulation*. 1998; 97: 1818–27.
43. **Oguchi S, Dimayuga P, Zhu J, *et al.*** Monoclonal antibody against vascular cell adhesion molecule-1 inhibits neointimal formation after periadventitial carotid artery injury in genetically hypercholesterolemic mice. *Arterioscler Thromb Vasc Biol*. 2000; 20: 1729–36.
44. **Gurtner GC, Davis V, Li H, *et al.*** Targeted disruption of the murine VCAM1 gene: essential role of VCAM-1 in chorioallantoic fusion and placentation. *Genes Dev*. 1995; 9: 1–14.
45. **Alam AK, Florey O, Weber M, *et al.*** Knockdown of mouse VCAM-1 by vector-based siRNA. *Transpl Immunol*. 2006; 16: 185–93.
46. **Leuker CE, Labow M, Muller W, *et al.*** Neonatally induced inactivation of the vascular cell adhesion molecule 1 gene impairs B cell localization and T cell-dependent humoral immune response. *J Exp Med*. 2001; 193: 755–68.
47. **Koni PA, Joshi SK, Temann UA, *et al.*** Conditional vascular cell adhesion molecule 1 deletion in mice: impaired lymphocyte migration to bone marrow. *J Exp Med*. 2001; 193: 741–54.
48. **Hogg N, Landis RC.** Adhesion molecules in cell interactions. *Curr Opin Immunol*. 1993; 5: 383–90.
49. **Carpen O, Pallai P, Staunton DE, *et al.*** Association of intercellular adhesion molecule-1 (ICAM-1) with actin-containing cytoskeleton and alpha-actinin. *J Cell Biol*. 1992; 118: 1223–34.
50. **Heiska L, Alfthan K, Gronholm M, *et al.*** Association of ezrin with intercellular adhesion molecule-1 and -2 (ICAM-1 and ICAM-2). Regulation by phosphatidylinositol 4, 5-bisphosphate. *J Biol Chem*. 1998; 273: 21893–900.
51. **Kansas GS, Pavalko FM.** The cytoplasmic domains of E- and P-selectin do not constitutively interact with alpha-actinin and are not essential for leukocyte adhesion. *J Immunol*. 1996; 157: 321–5.
52. **Weber C, Springer TA.** Interaction of very late antigen-4 with VCAM-1 supports transendothelial chemotaxis of monocytes by facilitating lateral migration. *J Immunol*. 1998; 161: 6825–34.